UNITED NATIONS UNIVERSITY
UNU-GTP
Geothermal Training Programme

Orkustofnun, Grensasvegur 9,
IS-108 Reykjavik, Iceland

Reports 2019
Number 22

BOREHOLE GEOLOGY OF WELL ThG-16 IN THEISTAREYKIR GEOTHERMAL FIELD, ICELAND

Vivi Dewi Mardiana Nusantara
PT. Pertamina Geothermal Energy
Skyline Building 19th floor, Jl. MH. Thamrin No. 9
Jakarta, 10340
INDONESIA
vivinusantara@pertamina.com

ABSTRACT

Well ThG-16 in Theistareykir geothermal field was drilled in 2017 and provides geological information from drill cuttings and logging data. The data is analysed in an integrated borehole geology study using multiple methods, such as binocular, petrography, X-ray diffractometry, the methylene blue dye adsorption test, and well logging interpretation. The objective of this study is to describe and interpret geological conditions in well ThG-16. The stratigraphy of the well is mainly composed of various hyaloclastite formations in the uppermost 1478 m. Between 1478 and 2290 m, lava flows are dominant and from 2290 m to the bottom of the well at 2702 m a coarse-grained intrusion zone is observed with dolerite and intermediate intrusions. The alteration zone is divided into five zones. From the surface to 80 m is an unaltered zone, followed by a smectite zone (80 – 170 m), a MLC zone (170-476 m), an epidote chlorite zone (476-1394 m), and an epidote chlorite actinolite zone (1394-2700 m). Three main feed points are observed in the well that are located at 2550-2590 m, 1980-2000 m, and 1450-1480 m. During drilling of well ThG-16 total loss of circulation was not experienced. It is suggested that the reservoir rock in the well has low permeability which is confirmed by the small size of fractures found in the televiewer log, the decreasing of good permeability mineral indicators as pyrite and calcite in the deeper part, and the long heating up period of the well after drilling.

1. INTRODUCTION

The Theistareykir geothermal field and power plant is situated in north Iceland. The field lies within the Theistareykir volcanic system in the Northern Volcanic Zone. The power plant units generated 90 MW installed capacity by the end of 2018 operated by the Icelandic national power company Landsvirkjun. The Theistareykir geothermal system lays within a fissure swarm trending NNE-SSW which is 7-8 km wide and about 80 km long. The Theistareykjahraun lava dates to c. 2400 BP and represents the most recent volcanic activity in the field (Saemundsson et al., 2007). Exploration drilling conducted since 2002 showed that the highest bedrock temperatures in the area are close to 380°C (Gautason et al., 2010).

Well ThG-16 was drilled by Iceland Drilling (Jardboranir) for Landsvirkjun in March 2017. The wellhead is located on pad C in the western foothills of Mt. Ketilfjall around 372 meter above sea level. ThG-16 is a 2702 m deep directional well with an azimuth of N 155° E and inclination angle of 35° (Gudjónsdóttir et al., 2017a).

Data from well ThG-16 provides geological information from cuttings, well logs, and drilling parameters. It is analysed conducting an integrated borehole geology study as it is strongly recommended for every completed well. This report presents the results of the borehole geology study in well ThG-16 with the objective to describe the current and past geological conditions in the borehole, using multiple methods like binocular, petrography, X-ray diffractometry, and the methylene blue dye adsorption test. In the end of the day, the result of this report can be used to support well ThG-16 production capacity assessment in the future with other multidisciplinary data.

1.1 Regional setting

Iceland consists of multiple volcanic systems resulting from the superposition of the spreading plate boundary and the mantle plume (Saemundsson, 1979; Hardarson et al., 1997). The Theistareykir geothermal field is one of the 5 main volcanic system formed by these regional activities and is located in the Northeast of Iceland (Saemundsson, 1974).

Saemundsson (2007) explained that the geology of Theistareykir consists of an east to west trending intrusion heat source with north – south trending permeable structures associated with the regional fissure swarm. The fissure swarm is trending NNE-SSW, is 7–8 km wide and about 60 km long. The geothermal surface manifestations are mostly confined to the eastern part of the fissure swarm, more specifically to the area northwest and north of Mt. Baejarfjall which is bounded by Theistareykjahraun lava to the west and Mt. Ketilfjall to the east. The geology map of the Theistareykir geothermal field is shown in Figure 1.

The surface in the Theistareykir field is mostly covered by lava flows. The older rock formations in this area are generally composed of hyaloclastites and pillow lavas. The most recent volcanic activity in the area occurred about 2400 years ago and the high-temperature geothermal activity is connected to recent magma intrusions (Saemundsson, 2007).

1.2 Drilling of well ThG-16

Well ThG-16 was designed as a step out well from pad C in the Theistareykir geothermal field. The drilling started on the 24th of March 2017 and finished on the 8th of May 2017 after a total of 46 operation days. The drilling contractor Iceland Drilling (Jardboranir) carried out the drilling operations with Landsvirkjun monitoring the work. Iceland GeoSurvey (ÍSOR) managed the cutting inspection, geophysical logging and geothermal consulting (Ásgeirsdóttir et al., 2017a; Ásgeirsdóttir et al., 2017b; Gudjónsdóttir et al., 2017a).

To reach the targeted faults and fissures beneath Mt. Baejarfjall, ThG-16 was designed as directional well with an azimuth of 155° ± 5° relative to true north, the inclination value was set around 35° ± 3°, the kickoff point (KOP) was located at 400 m, the end of built (EOB) at 850 m, and total depth of the well is 2702 m (Gudjónsdóttir et al., 2017a). Location and trajectory of well ThG-16 is shown in Figure 2.

ThG-16 was drilled by the Ódinn rig. All the depth measurements are relative to a reference point 6.8 meter above ground level which is Ódinn's rig floor. Table 1 below shows the configuration of the borehole, casing design, and types of data retrieved from the different sections.

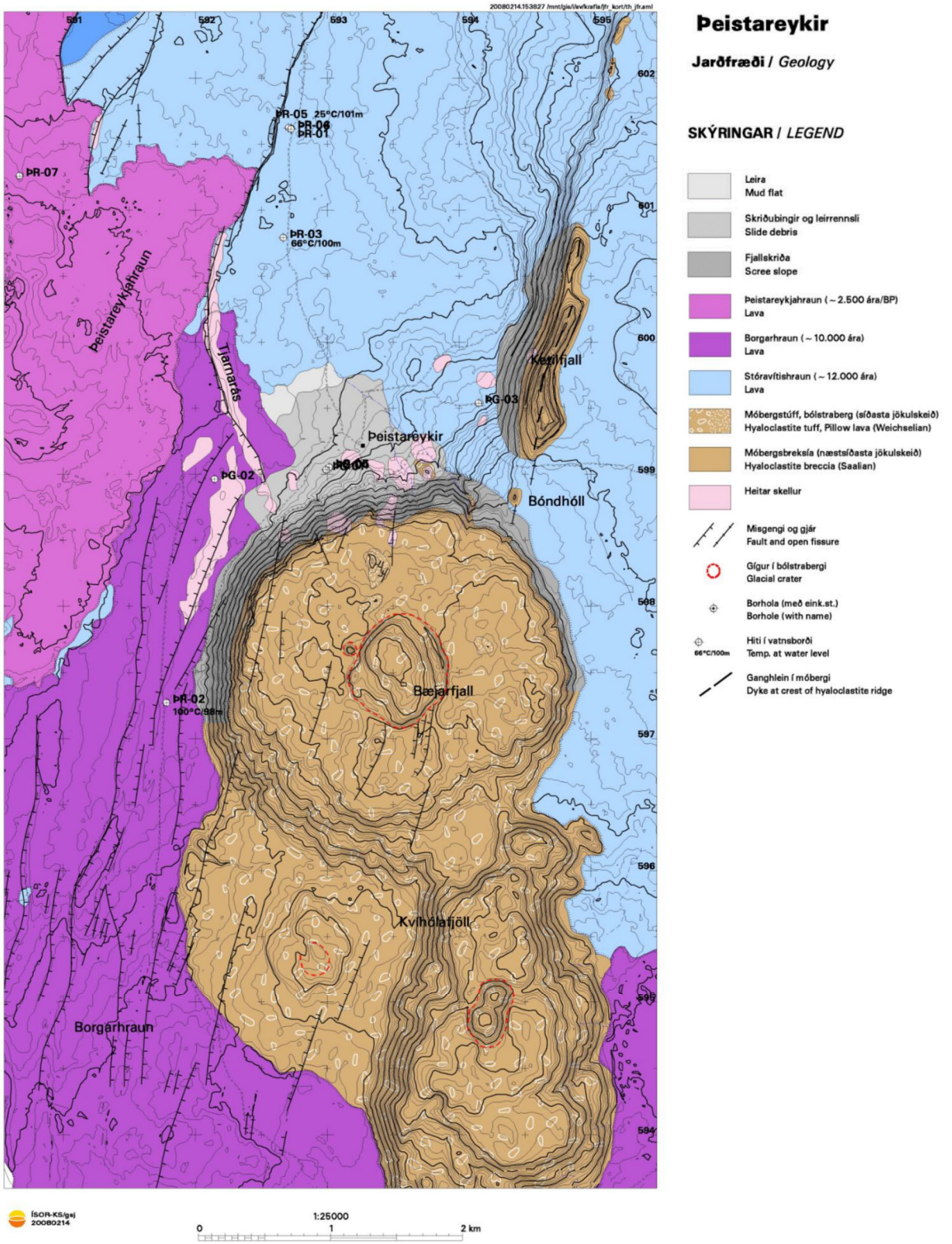

FIGURE 1: Geological map of the Theistareykir geothermal field showing surface rock dominantly composed from lava and hyaloclastite formations (Saemundsson, 2007)

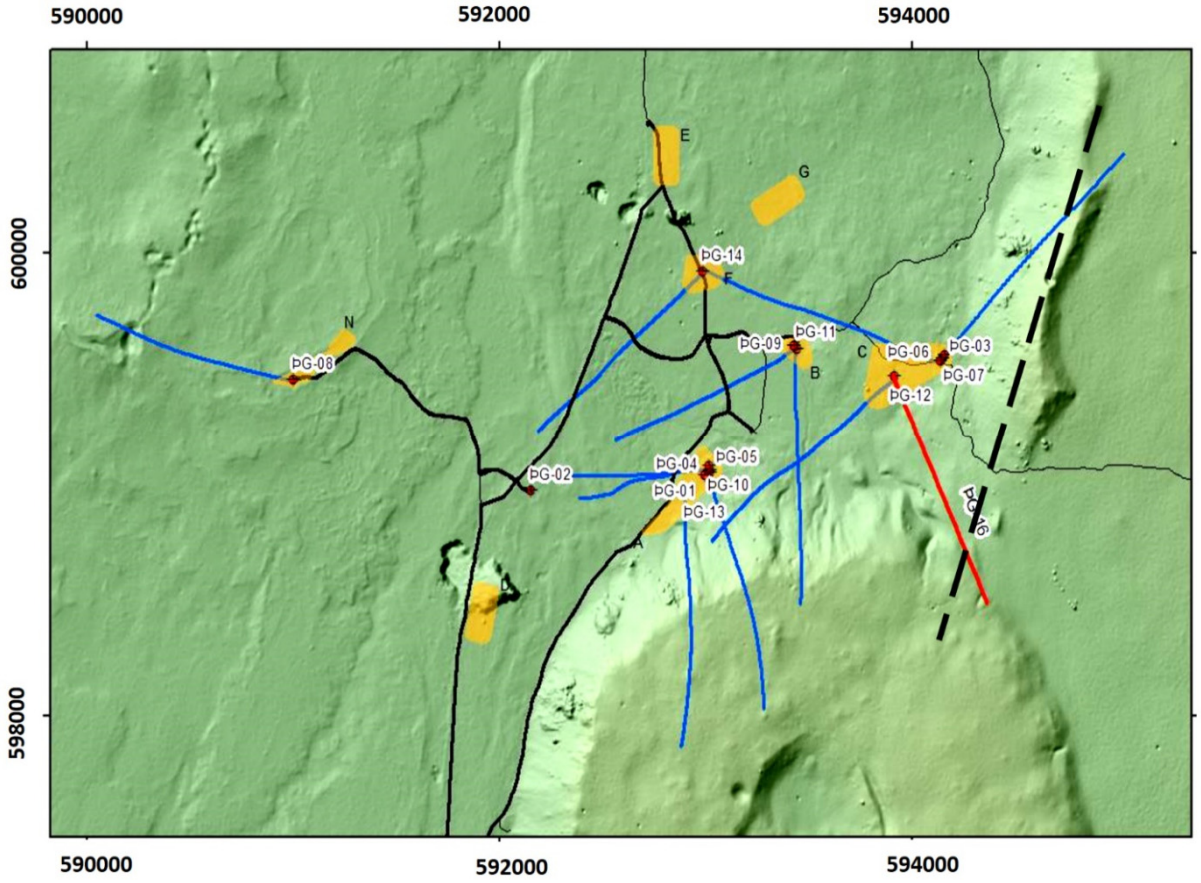

FIGURE 2: Location of production wells in the Theistareykir area. Trajectory of well ThG-16 is shown as a red line located in well pad C drilled directed relatively to Mt. Baejarfjall (Gudjónsdóttir et al., 2017a)

TABLE 1: Casing design and data retrieved from well ThG-16 (Gudjónsdóttir et al., 2017a)

Phase	Drill bit	Casing type	Casing shoe depth	Data retrieved
0	21"	18 5/8"	118 m	Cuttings, drill parameter, PT, CBL.
1	17 ½"	13 5/8"	303 m	Cuttings, drill parameter, PT, CBL, NN.
2	12"	9 5/8"	854 m	Cuttings, drill parameter, PT, CBL, NN, caliper, resistivity.
3	8 ½"	7" perfor. liner	2702 m	Cuttings, drill parameter, PT, NN, caliper, resistivity, gyro, gamma, acoustic, spinner and injectivity.

*PT: Pressure-Temperature, CBL: Cement Bond Log, NN: Neutron Neutron.

Well ThG-16 encountered only minor loss of circulation during drilling. The losses were 0 to 5 l/s down to 2313 m but during a change of drill bit at that depth the loss increased to 15 l/s and stayed between 9 and 15 l/s for the rest of the drilling. All the feed points are considered small to moderate in size. The most permeable feed points are located at 1450-1480, 1980-2000 and 2250-2590 m (Ásgeirsdóttir et al., 2017a; Gudjónsdóttir et al., 2017a).

2. METHODS AND DATA PROCESSING

Cuttings and well logs are the main data retrieved from well ThG-16 which is thoroughly analysed in this study. Cutting samples were collected every 2 meters from the surface to 2702 m depth. Several well logs data such as temperature, calliper, resistivity, neutron – neutron (N-N), and gamma are used in this analysis. All the data mentioned above was published as a final well report by ÍSOR for Landsvirkjun (Gudjónsdóttir et al., 2017a).

Various standard rock cutting analysis methods were applied in the geology study. They were carried out in sequence, starting with binocular analysis, petrography analysis, X-ray diffractometry (XRD) measurement, and the methylene blue dye adsorption test.

Binocular analysis is a quick method to identify rock types and mineralogy in megascopic scale. It is carried out onsite by wellsite geologists and re-observed later in the laboratory for more detailed results. In the petrography analysis a polarizing microscope is used to examine thin section samples of cuttings from specific depths. It is one of the most basic methods to examine the micro-optic properties of individual minerals in detail and amount. It is relatively affordable, fast and accurate.

X-ray diffractometry (XRD) is used when the particles to be identified are too small to be clearly resolved with the microscope, such as clay particles, or when minerals exist as solid solutions or mixtures (Chen, 1977). Three types of XRD analysis were carried out using crushed powder cutting samples called clay treated analysis. Clay treated analysis includes clay measurements. The samples are treated in three different was: air dried, put in a container with ethylene glycol and heated. Every clay mineral show as a different peak in the XRD treatment. Clay mineral identifications were made by air drying and glycolation of the samples to identify smectite by its expandable shifted peak at 15 angstroms. The clay samples were heated to 550°C to distinguish between kaolinite and chlorite which both have a peak at 7 angstroms. The peak of kaolinite will be destroyed during the heating.

The methylene blue dye adsorption test (MBT) is a semi quantitative method to determine the amount of swelling clay (mainly smectite) in rocks and soil materials. A decreased amount of swelling clay indicates a higher alteration rank, typically in the reservoir zone. A high amount of swelling clay generally correlates with low thermal conductivity (Nehler et al., 2014).

3. RESULTS

3.1 Borehole stratigraphy of well ThG-16

The rock types are identified using binocular and petrography analysis and displayed as a detailed lithology log. By grouping the lithology types based on their dominant facies, borehole stratigraphy zones are produced. Borehole stratigraphy zones of well ThG-16 are simplified and explained in Figures 3 and 4.

From the borehole geology log, different lithologies can be grouped into stratigraphy zones. Each stratigraphy zone, its depth and characteristics are explained below.

10 – 66 m, Lava flow zone. This zone is the shallowest zone retrieved from the cutting data. It shows an intercalation of fresh basaltic lava mixed with scoria and reworked sedimentary rocks. The basalt has a porphyritic texture with plagioclase and olivine phenocrysts and glassy mafic material as groundmass. Some rock fragments are reddish to dark grey with vesicle structures in the rock mass while oxidation and alteration rank is low.

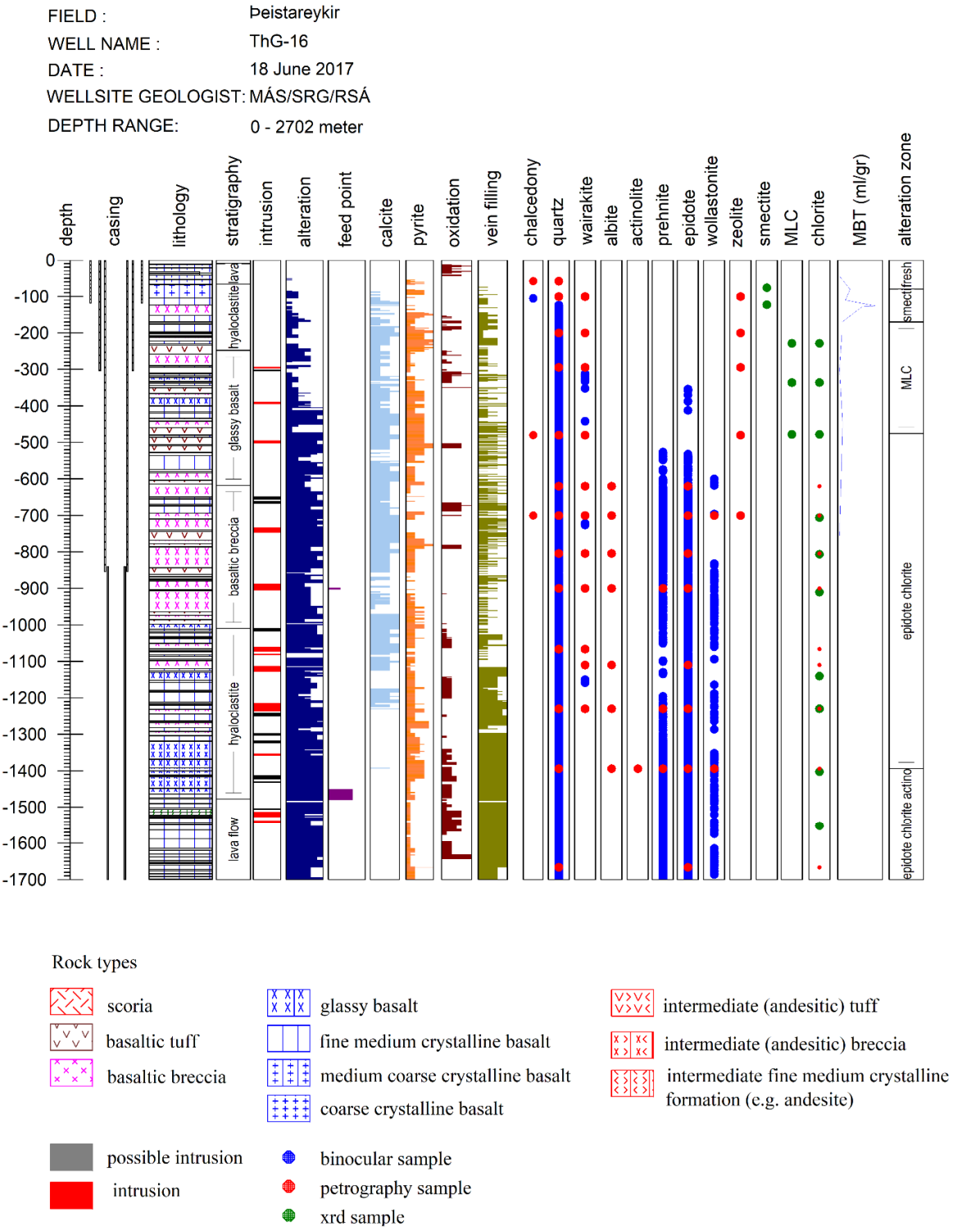

FIGURE 3: Borehole geology log of well ThG-16 from 0 to 1700 m notifies the information about lithology unit, stratigraphy, alteration, intrusion, feed zones, and mineral distribution in the well (modified from Gudjónsdóttir et al., 2017a)

66 – 248 m, Hyaloclastite zone. The hyaloclastite zone consists of greenish fine-grained tuff and tuff breccia layers. The rock texture is fragmental with evidence of flow texture. Some samples show pumicious structures which are found around open vesicles. Brownish clay minerals are found in the rock matrix with some secondary mineral deposits like pyrite, calcite, wairakite, chalcedony, and secondary quartz. This zone has a low rank of alteration and is moderately oxidized.

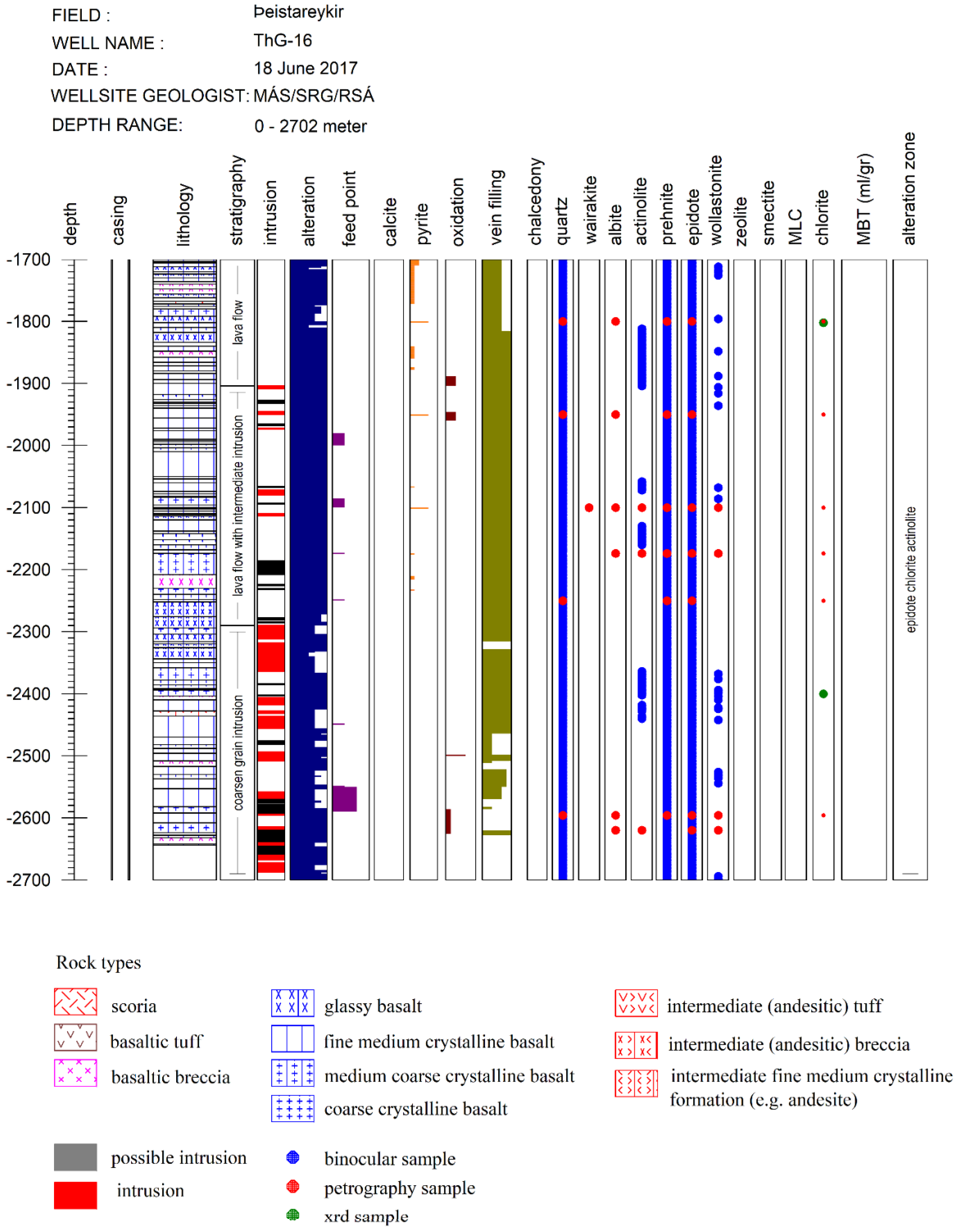

FIGURE 4: Borehole geology log of well ThG-16 from 1700 to 2700 m notifies the information about lithology unit, stratigraphy, alteration, intrusion, feed zones, and mineral distribution in the well (modified from Gudjónsdóttir et al., 2017a)

248 – 618 m, Glassy basalt zone. In this zone there are some intrusive dolerite and pillow lava flows between glassy basalt formations. Plagioclase, pyroxene, and olivine are altered to MLC and chlorite, calcite, zeolite, wairakite, dispersed pyrite, chalcedony, and secondary quartz. Epidote and prehnite start to appear from 530 m depth. This zone varies from the upper part by its high intensity of alteration and oxidation. The rock formation is fractured, rich in veins, and porous.

618 – 1010 m, Basaltic breccia zone. This zone is composed of greenish to dark brown basaltic breccia, mixed with tuff fragments, hyaloclastite, and intermediate coloured rocks. Minerals like pyroxene, plagioclase, and the glassy aphanitic mass are highly oxidized and altered. Secondary mineral such as epidote, pyrite, wollastonite, wairakite, and prehnite are abundant. The rock is fractured with vein filling. Chlorite abundance is increasing from 620 m. Intrusion were spotted at 650, 662, 734, and 742 m.

1010 – 1478 m, Hyaloclastite zone. This zone of tuff rich hyaloclastite consists of intercalations of greenish grey coloured tuff, glassy fine-grained basalt, and tuff breccia, with dolerite intrusion spotted at several depths (1010 m, 1062 m, 1080 m, 1114 m, 1216 m, 1242 m, 1298 m, 1318 m, 1354 m, 1414 m, 1430 m). The formation is highly altered and low oxidized. The rock vesicles are filled by epidote, wollastonite, wairakite, chlorite, prehnite, pyrite, albite, quartz, and calcite.

1478 – 1904 m, Lava flow zone. The lava flow zone has a porphyritic texture in its rock composition of glassy fine-grained basalt and tholeiitic basalt intrusions. The formations is mostly dark grey, reddish, and greenish to brownish grey. Secondary minerals such as wollastonite, actinolite, chlorite, and epidote are abundant. Pyrite is hardly found in this zone. This zone is highly altered with low to medium rank of oxidation. Vein fillings are intense, but the presence of open vesicles is minor.

1904 – 2290 m, Lava flow with intermediate intrusion zone. This zone is mostly composed of lava flows with intercalation of fine to medium-grained glassy basalt. Intrusion rocks encountered are identified by thin section analysis as dolerite. The alteration rank is high in this formation, it is abundant in veins, but lack vesicles. Secondary minerals are composed of wollastonite, actinolite, prehnite, epidote, chlorite, and secondary quartz. This zone lacks pyrite and there is no evidence of calcite which might indicate low permeability and the lack of calcite could also be an indicator of temperatures above the mineral´s forming temperature of 260°C. Intrusions are common in this interval.

2290 – 2702 m, Coarse-grained intrusion zone. This zone consists of coarse-grained basalt and dolerite with typical ophitic and subophitic texture. The rock formation is highly altered and has low porosity. This is followed by a decreasing amount of vein filling in dolerite cutting chips compared to the lava zone above 1904 m. High-temperature minerals like actinolite, epidote, prehnite, quartz, and chlorite are found a lot in thin section samples.

3.2 Intrusion rocks in well ThG-16

Intrusion rocks in well ThG-16 are identified by using multiple analysis techniques. The results are interpreted together with the results obtained from the binocular analysis, wire line logs (resistivity, neutron – neutron, gamma), and petrography analysis. The log is shown in Figure 5. Table 2 summarizes the intrusion rocks that are discovered in the borehole.

Some intrusions were strongly confirmed by petrography analysis. The crystals form phaneritic texture with coarse sized euhedral phenocrysts as the main composition. These phenocrysts are composed of plagioclase, pyroxene, and olivine. Olivine and pyroxene crystals were altered to epidote and chlorite while plagioclases were altered to epidote and albite (Figure 6).

Dolerite in well ThG-16 was identified by its ophitic – subophitic texture between plagioclase with olivine and pyroxene (Figure 7). Ophitic texture refers to envelopment of plagioclase laths by larger clinopyroxenes. It is commonly interpreted to indicate that the clinopyroxenes formed later in dolerite. Subophitic texture is formed when the feldspar crystals are approximately the same size as the pyroxene and are only partially included by them (MacKenzie et. al., 1982).

Figure 7 shows the subophitic texture that observed in thin section sample of cutting from well ThG-16 at 1950 m. In a crossed polarized light picture (Figure 7 left), subhedral clinopyroxene crystals have a first order yellow to red and purple in colour, with a positive relief. Plagioclase crystals show twinning

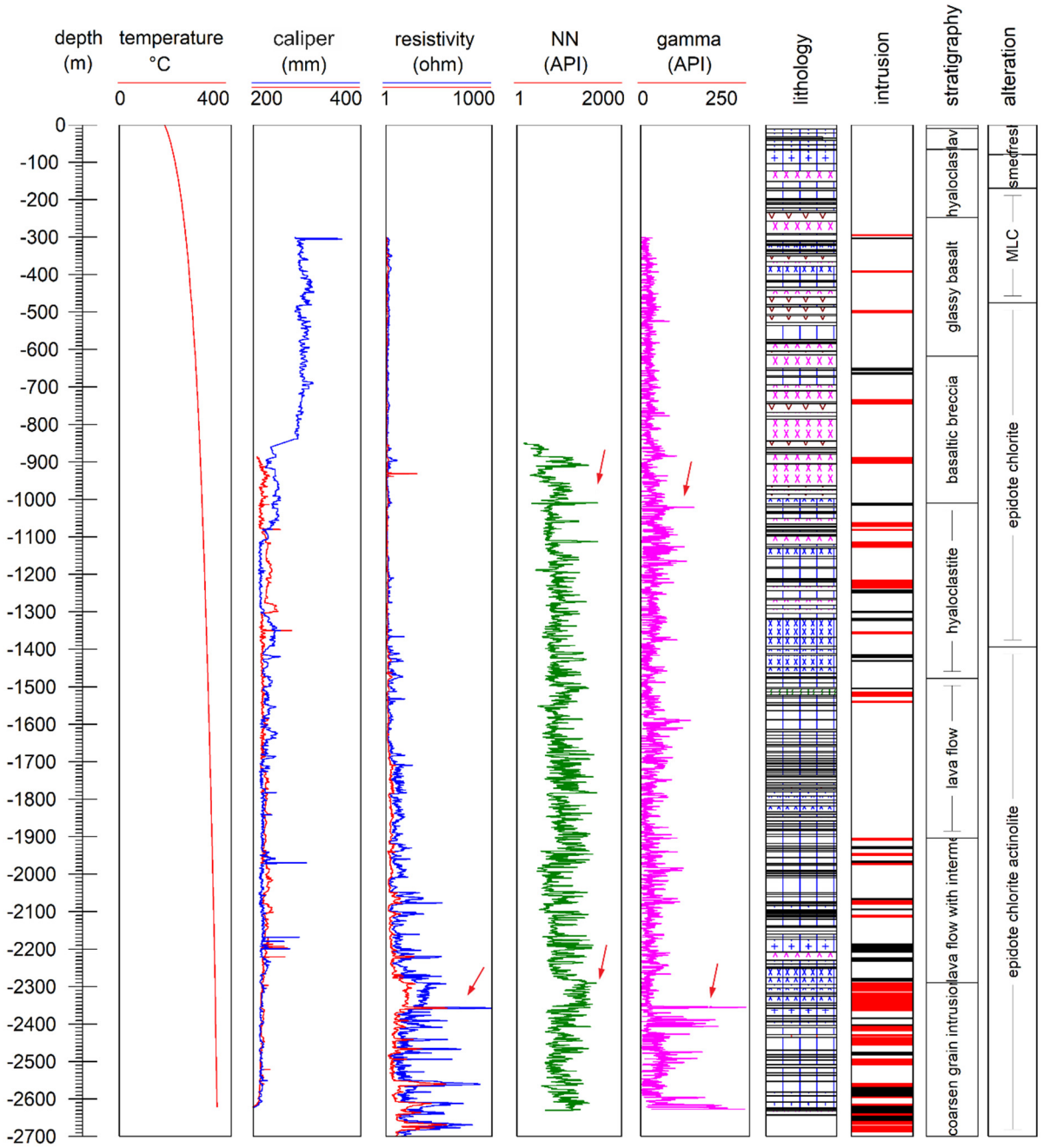

FIGURE 5: Multiple wire line log used to define intrusion rocks in borehole ThG-16. The intrusions are identified as coarse-grained basalt and dolerite that show a typical high response in resistivity, neutron, and gamma. From 2290 m, these intrusions become thicker and are frequently encountered. Red arrows show the typical spike of highly anomaly response that indicate the presence of intrusions

structure in white to dark grey colour. In plane polarized light picture (Figure 7 right), clinopyroxene has white to yellowish colour with pleochroic feature from greenish white to colourless. This is caused by the content of iron (Fe) in its composition. In the other hand, plagioclase is colourless, and does not have pleochroism. Both minerals have relatively the same coarse crystal size that defined as subophitic texture.

TABLE 2: Intrusion group in ThG-16 interpreted from logging and sample analysis results

Intrusion zone	Top	Bottom	Evidence	Remarks
Shallower group intrusion	294	746	No logging data above 303 m. Low response in logging data below 303 m but confirmed by binocular and petrography check.	Blackish fine-grained fresh dense basalt and dolerite with ophitic and subophitic texture. The intrusions in this zone are associated with glassy basalt and basaltic breccia layers. The thickness of each intrusion layer is around 2 m.
Middle group intrusion	888	1542	Fluctuating response in neutron and gamma log. The result is conformable with rock analysis which identified the rock as intrusion.	Composed of crystalline basalt and dolerite mixed with brownish tuff and breccia fragments. This zone is associated with hyaloclastite formation. The thickness of each intrusion layer is between 4 and 12 m.
Deeper group intrusion	1542	2208	Logging data response is medium to high in this zone. Feed points are mostly found in this interval.	Basalt and dolerite are highly altered, associated with chlorite and lava flow formation. The thickness of intrusion layers are around 2 – 4 m.
Deep seated intermediate intrusion body	2208	2688	Extremely high response in resistivity and gamma log. Feed points found abundant in this interval.	Frequent appearance of crystalline coarse-grained basalt and dolerite. The intrusion layers become thicker, up to 20 m in the deeper part.

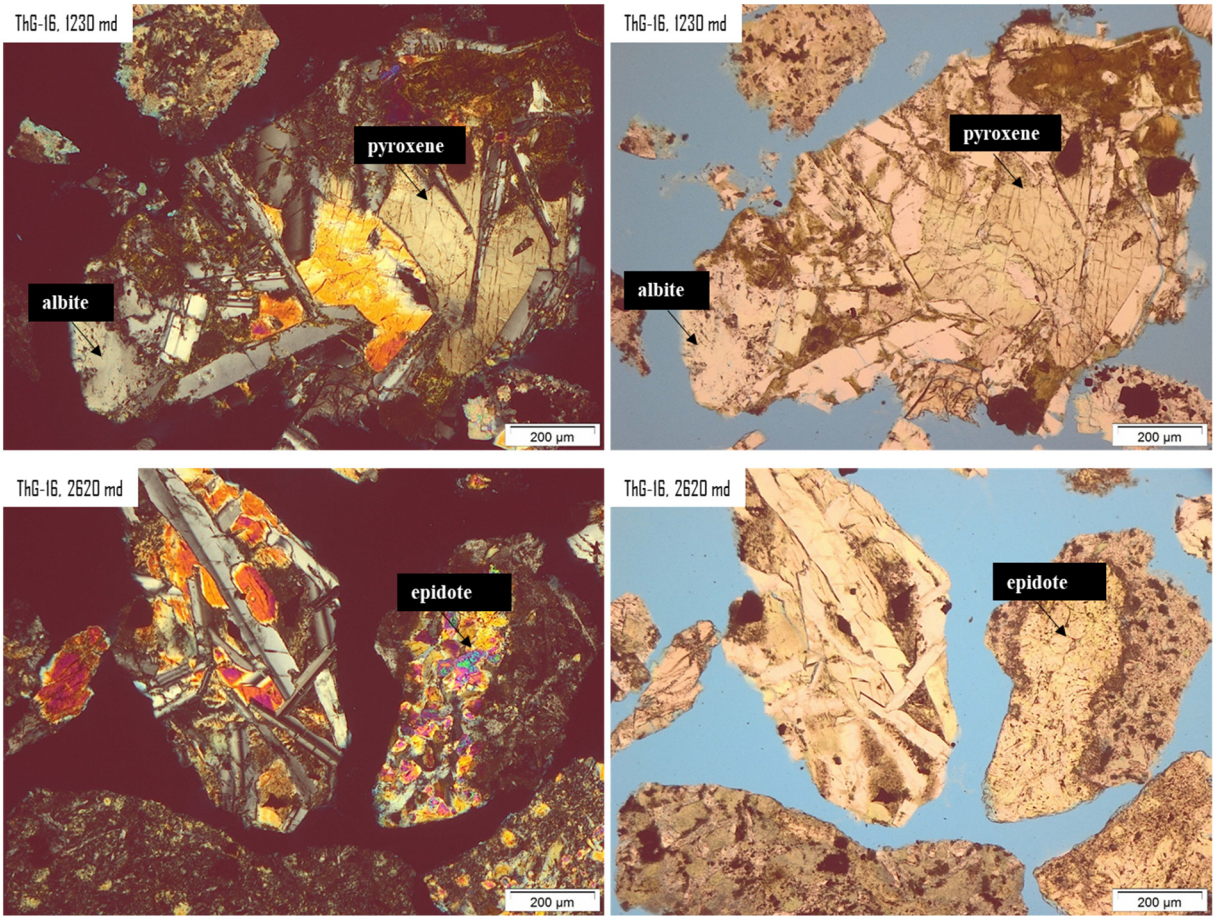

FIGURE 6: Intrusion rocks identified at 1230 m (upper figure) and 2620 m (lower figure) in well ThG-16 show that dolerite and coarse crystalline basalt with plagioclase and pyroxene as phenocrysts were altered to high temperature secondary minerals like epidote and albite

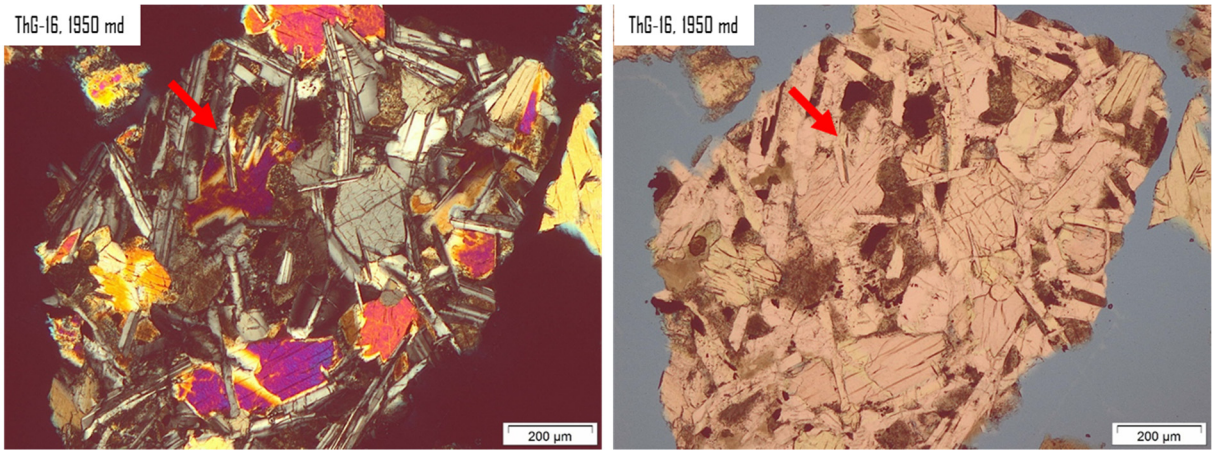

FIGURE 7: Dolerite intrusion from well ThG-16 at 1950 m show subophitic texture between clinopyroxene and plagioclase crystals (red arrow)

3.3 Hydrothermal alteration in well ThG-16

Alteration mineralogy documents the post formation history of the rock where the rock forming minerals (primary) are altered into secondary alteration minerals. Since they are a product of geothermal activity, these secondary minerals provide information of reservoir and fluid characteristics and the evolution of geothermal system (Thompson and Thompson, 1996).

Hydrothermal alteration minerals in well ThG-16 are a product of hot water – rock interaction caused by geothermal activity. These secondary minerals were identified by binocular, petrography, and X-ray diffractometry (XRD) analysis. Some of the secondary minerals fill the vesicles and veins as fluid deposition product or are replacing the existing phenocryst and groundmass of the rock. Table 3 shows the distribution of primary and secondary minerals that were observed by petrography analysis.

3.3.1 Alteration minerals in well ThG-16

Distribution of alteration minerals in well ThG-16 were plotted together with the borehole geology log of well ThG-16 in Figure 3 and 4 and described in Table 3. Some factors affect the formation of hydrothermal minerals which are related to, e.g. temperature, pressure, rock type, permeability, fluid composition, and duration of hydrothermal exposure (Browne, 1978). Each secondary mineral and its significance to predict subsurface geological conditions in the well is explained below:

Calcite. Calcite was mostly found between 86 and 1230 m and is characterized by its optical properties of high relief and strong birefringence under petrography analysis. Calcite fill the veins and vesicles in the rock formation. Its abundance and distribution are associated with wairakite.

Pyrite. Pyrite is a sulphide mineral and its presence is often an indicator of good permeability. This mineral was constantly identified from 54 m depth onwards until it gradually disappeared below 1774 m and was not observed below 2200 m. Pyrite was found as vein-fillings and dispersed in the rock's groundmass.

Iron oxide. Iron oxide colours the rock reddish due to its iron (Fe) content. It is commonly formed during the altering high ferrous mineral like olivine and pyroxene in basaltic rock. Iron oxide zones were found almost continuously from the surface down to 1636 m, but traces of oxidation were found sparsely down the well.

TABLE 3: Summary of mineralogy distribution in well ThG-16 identified in petrography analysis

No.	Depth (md)	Lithology	Primary mineral	Secondary mineral	Mineral sequence	Remarks
1	58	Mix fresh basalt, basalt olivine, tuff, pumice.	gls, plg, olv, px, opq.	opq, io, chal.	clay – chal.	Flow texture, pumicious. Highly porous with open vesicular features, little vein evidence found
2	100	Basalt	gls, plg, olv, px, opq.	cal, opq, io, qz, wai. zeo.	zeo - cal	Glassy, pillow lava, lack of vesicle and low amount of veins evidence found
3	200	Tuff	gls, fine grain feldspar, opq.	cal, opq, qz, wai, zeo.	zeo – cal – qz. qz – wai.	Vesicles and veins quite abundant filled by clay alteration minerals
4	294	Dolerite intrusion	plg, olv, px, opq.	cal, opq, io, qz, wai, zeo.	qz - cal	Massive, lack of vesicles and veins, subophitic
5	480	Tuff	gls, plg, opq.	cal, opq, io, chal, qz, wai, zeo.	zeo – cal. cal – wai.	Veins abundant
6	620	Basalt	plg, olv, px, opq.	cal, opq, io, qz, wai, alb, ep, chlo.	qz – cal. chlo – ep – cal.	Veins abundant
7	700	Basalt	plg, px, opq.	cal, opq, io, chal, qz, wai, alb, ep, wol, zeo, chlo.	cal – qz – ep.	Crystalline, veins abundant
8	804	Tuff	gls, plg, opq.	cal, opq, io, qz, wai, alb, preh, ep, chlo.	io – qz. ep - chlo	Replacement of plagioclase by epidote, veins abundant, phenocrysts replaced
9	900	Dolerite intrusion	gls, aphanitic mass, fine feldspar, opq.	cal, opq, io, qz, wai, alb, preh, ep, chlo.	ep – qz – preh.	Ophitic, veins abundant, mineral deposition in rock mass
10	1066	Basalt	gls, aphanitic mass, fine feldspar, opq.	cal, opq, qz, wai, chlo.	cal – wai – chlo.	Highly vesicular and fractured with veins
11	1110	Hyaloclastite	gls, plg, opq.	cal, opq, wai, albm ep, chlo.	chlo – cal. alb – cal.	Rich in albitization and chloritization
12	1230	Dolerite intrusion	plg, px, olv, opq.	cal, opq, io, qz, wai, alb, preh, ep, chlo.		Phaneritic, subophitic, fractured filled by veins
13	1394	Basalt	plg, px, olv, opq.	cal, opq, qz, alb, act, preh, ep, wol, chlo.		Crystalline
14	1666	Tuff breccia	gls, opq.	opq, qz, ep, chlo.	qz – ep.	
15	1800	Basalt	plg, px.	qz, alb, preh, ep, chlo.		Porphyritic, fractured filled by veins
16	1950	Dolerite intrusion	plg, px, olv.	qz, alb, preh, ep, chlo.		Ophitic texture
17	2100	Lava basalt	gls, plg.	wai, alb, act, preh, ep, wol, chlo.		Rich in veins and vesicular
18	2174	Glassy basalt	ls, plg, px.	alb, act, preh, ep, wol, chlo		Porphyritic
19	2250	Tuff	gls, plg.	qz, preh, ep, chlo.	qz - ep	Veins decreasing
20	2596	Basalt intrusion	plg, px.	qz, alb, preh, ep, wol, chlo.		
21	2620	Dolerite intrusion	plg, px, olv.	alb, act, ep, wol, chlo.		Phaneric, subophitic
Abbreviation: gls: glass, plg: plagioclase, px: pyroxene, olv: olivine, opq: opaque, cal: calcite, io: iron oxides, chal:chalcedony qz: secondary quartz, wai: wairakite, alb: albite, act: actinolite, preh: prehnite, ep: epidote, wol: wollastonite, zeo: zeolite, chlo: chlorite.						

Chalcedony. Chalcedony is usually associated with secondary quartz around fractures or veins within permeable zones at relatively shallow levels (Thompson and Thompson, 1996). In this well, chalcedony is spotted at 58, 104, 480, and 700 m. Its distribution resemblance zeolite which indicates a low-

temperature zone (40-120°C). While chalcedony only appears at shallower depth, secondary quartz is continuously visible down to 2700 m.

Secondary quartz. Secondary quartz indicates rock temperatures higher than 180°C (Reyes, 2000). Secondary quartz is encountered in the entire well (58 – 2700 m). Secondary quartz was mostly found as pore and vein-filling.

Wairakite. Wairakite is formed at a minimum temperature of 200°C in neutral pH conditions (Reyes, 2000). In well ThG-16, wairakite was semi-continuously found from 100 to 1230 m. Mostly, the mineral appeared as pore and vein fillings and was observed in association with calcite, quartz, chlorite, and epidote.

Albite. Albite is generally stable at 150 to 220°C as an alteration mineral (Reyes, 2000). In ThG-16, albite was observed in thin sections from 620 m and in increasing amounts in the deeper parts of the well. It replaced compositions of feldspar especially plagioclase at 620, 700, 804, 900, 1230, 1394, 1800, 1950, 2100, 2174, 2596, and 2620 m.

Actinolite. Actinolite indicates formation temperatures above 280°C (Kristmannsdóttir, 1979). In ThG-16 it starts to appear at around 1394 m depth in tiny needle like form (first detected in thin section) and becomes more abundant at around 1812 m and deeper, both observed in thin section and drill cutting analysis. The actinolite distribution is associated with other high-temperature minerals like epidote and chlorite. Actinolite is shown in Figure 8. In a crossed polarized light picture (upper left in Figure 8), actinolite has a high second order interference colour of yellow, red, green to greenish blue. Its

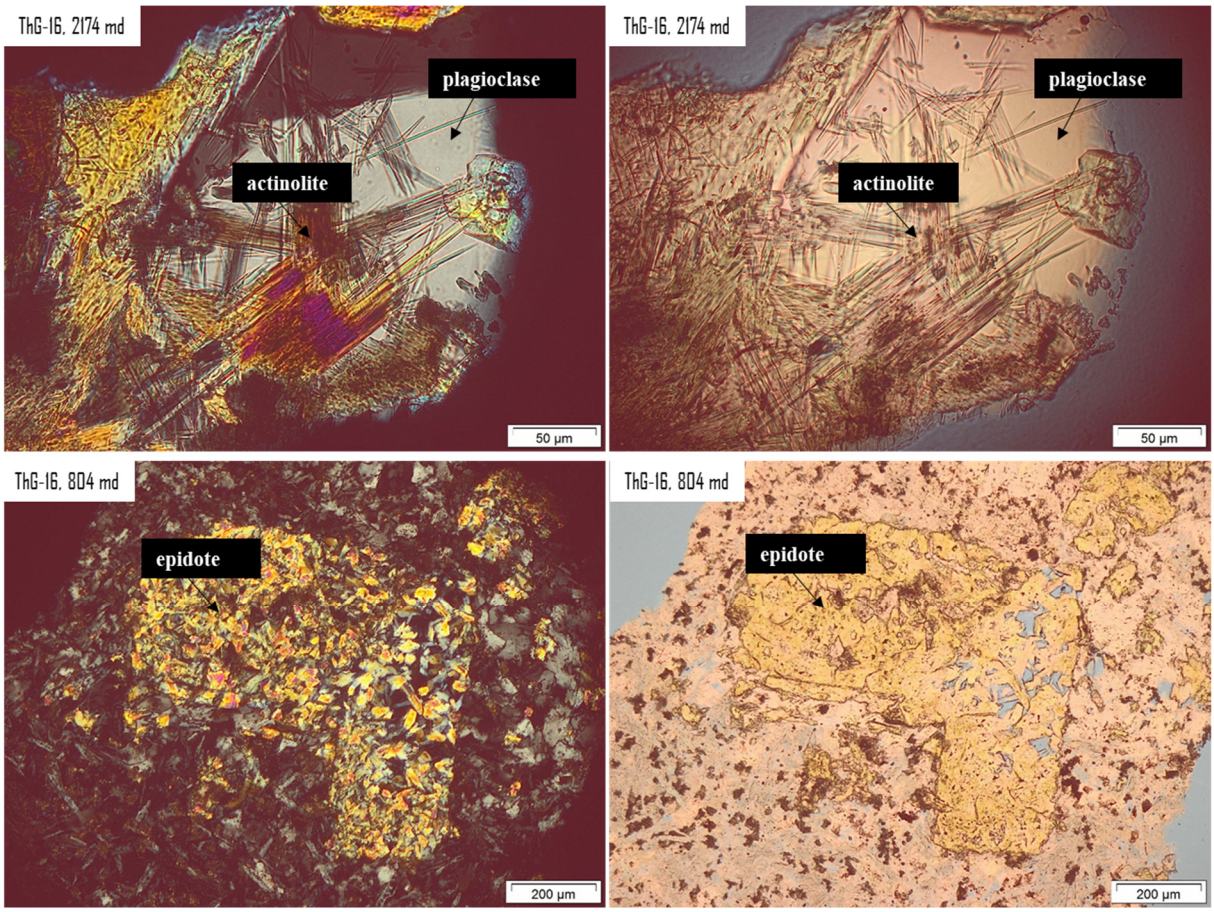

FIGURE 8: Photomicrograph of neutral high temperature secondary mineral found in well ThG-16. At 2174 m (upper figures) actinolite crystal grows in needle like form that overlays plagioclase. At 804 m (lower figures) epidote completely replaced primary mineral crystals (possibly plagioclase)

distinguished by its needle like form and high relief. It has pleochroism from colourless to green which is visible on plane polarized light condition (Figure 8 - upper right).

Prehnite. Prehnite is formed in high-temperature condition above 220°C (Reyes, 2000). Prehnite appears in ThG-16 below 526 m and is seen in binocular analysis of the drill cuttings continuously down the well. It is commonly associated with secondary quartz and epidote (Figure 9). Prehnite shows a prismatic to fanlike crystal shape. In crossed polarized light picture (Figure 9 - left), prehnite shows interference colour of strong yellow to reddish yellow. In contrast, it is colourless to pale yellow when its observed under plane polarized light (Figure 9 - right).

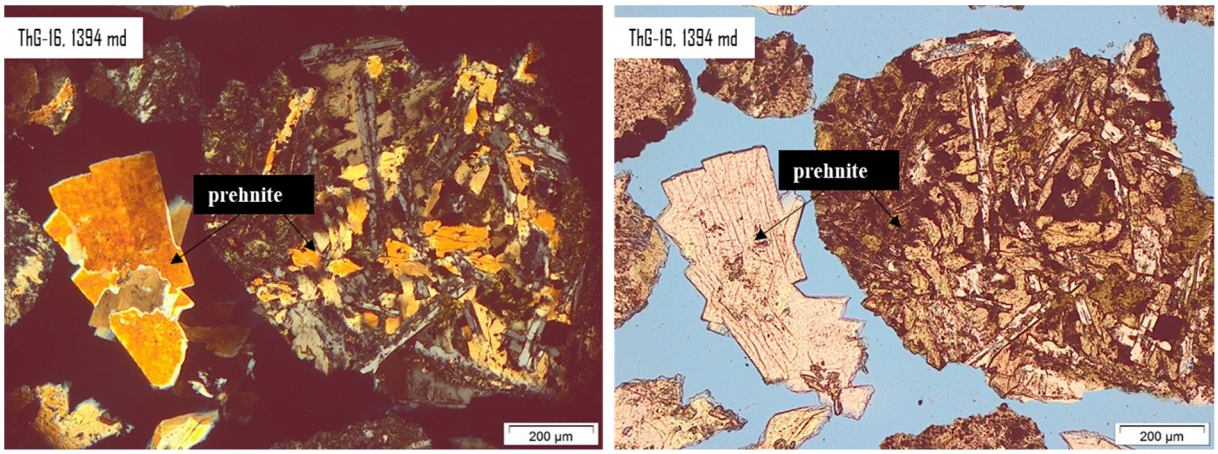

FIGURE 9: Photomicrograph of prehnite in well ThG-16 at 1394 m

Epidote. Epidote is formed at a minimum temperature of 230°C (Reyes, 2000). In well ThG-16 traces of epidote appear in binocular analysis of the drill cuttings at 354 m and increase consistently below 532 m. Well grown euhedral prismatic epidote replaces primary minerals, fills the veins and vesicles in the rock. These euhedral epidote crystals are clearly observed by petrography sample analysis at depth 620, 700, 804, 900, 1066, 1110, 1230, 1394, 1666, 1800, 1950, 2100, 2174, 2250, 2596, and 2620 m. Epidote as a secondary mineral is shown in Figure 8. Epidote in crossed polarized light picture (Fig. 8 lower left) has a high order of interference colour from yellow, yellowish green, to yellowish red of the second order. It has strong pleochroism in plane polarized light (Figure 8 lower right) from yellow to dark green colour that formed inside of the replaced primary crystal cast (possibly plagioclase).

Wollastonite. Wollastonite indicates high reservoir temperatures above 260°C (Helgadóttir et al., 2010). Wollastonite was observed from 600 m and deeper. The first occurrence of wollastonite was found in almost the same horizon as the first occurrence of chlorite (see chlorite below).

Zeolite. In Icelandic geothermal systems low-temperature zeolites and amorphous silica form below 100°C (Kristmannsdóttir, 1979). Zeolite is visibly observed from petrography analysis starting from 100 m depth and disappears at 700 m.

Smectite. Clay minerals like smectite crystallize below 200°C (Kristmannsdóttir, 1977). Smectite is hardly seen in the binocular and petrography analysis. XRD data suggests that a smectite zone is located between 80 and 170 m depth, conformable with swelling test by methylene blue dyed analysis (see Figure 3).

Mixed layer clay (MLC). MLC forms at 200-230°C (Kristmannsdóttir, 1977). A MLC zone is found around 170 - 476 m with interlayers of smectite – chlorite clays.

Chlorite. Chlorite forms above 230°C (Kristmannsdóttir, 1977). Chlorite identified from petrography analysis starts to appear from 620 m and was found in spot samples down to 2700 m.

Specifically, for the clay group mineral, the combination of XRD and methylene blue dye adsorption test (MBT) is used to identify fine clay group minerals like smectite, chlorite, and mixed layer clay (MLC).

15 cutting samples were analysed for clay using the XRD method from the shallower to deeper part of the well to observe the variation of clay type minerals which are commonly associated with the temperature distribution. The samples were measured in three steps: air dried, glycolated, and heated up to 550°C. Interpretation is made by picking the peak of each mineral. The same mineral assemblages are grouped into zones and plotted along the well based on its clay type. All of them are summarized in Table 4 below.

From Table 4, three types of clay mineral were identified. At shallower depth, smectite appears from 76 to 122 m. Smectite is characterized by its peak at ~15 Å when air dried. By adding ethylene glycol, the peak position shifted from ~15 Å to ~17 Å. After heating, the smectite peak decayed to ~10 Å (Figure 10a).

Mixed layer clay (MLC) in well ThG-16 was composed of chlorite – smectite layers. It shows a strong peak at ~14 and ~7 Å. These peaks increase after the glycol treatment with a reflection peak at around 28 to 32 Å. This zone is found from 228 to 478 m depth (Figure 10b).

Chlorite shows a strong peak at ~7 and ~14 Å when the sample is dried and treated with the glycol solution. The strong peak remains relatively the same when the sample is heated up to 550°C showing that the chlorite is stable from 706 to 2400 m (Figure 10c).

An amphibole peak was identified at 1140 m at 8.5 and 8.6 Å. At 2100 m no clear peak can be observed, probably due to lack of clay content in the rock composition at this depth which is composed of lava basalt based on petrography observation.

TABLE 4: The result of X-ray diffractometry (XRD) clay treatment analysis for well ThG-16

No.	Depth (m)	d(001) untreated (Å)	d(001) glycolated (Å)	d(001) heated (Å)	d(002)	Type of clay
1	76	15.2	15.7	10.1	0	Smectite
2	122	15.5	17.5	10.1	0	Smectite
3	228	14.3	14.3	14.3	7.2	MLC, unstable chlorite
4	336	14.6	14.6	14.6	7.2	MLC, unstable chlorite
5	478	14.5	14.5	14.5	7.1	MLC, unstable chlorite
		10.2	10.2	10.2	0	Illite
6	706	14.7	14.7	14.7	7.2	Chlorite
7	806	14.6	14.6	14.6	7.2	Chlorite
8	910	14.6	14.6	14.6	7.2	Chlorite
9	1140	14.6	14.6	14.6	7.2	Chlorite, amphibole,
		10.3	10.3	10.3	10.3	Illite
10	1230	14.7	14.7	14.7	7.2	Chlorite
11	1402	14.6	14.6	14.6	7.2	Chlorite
12	1552	14.5	14.5	14.5	7.1	Chlorite
13	1802	14.8	14.8	14.8	7.2	Chlorite
14	2100					
15	2400	14.8	14.8	14.8	7.2	Chlorite

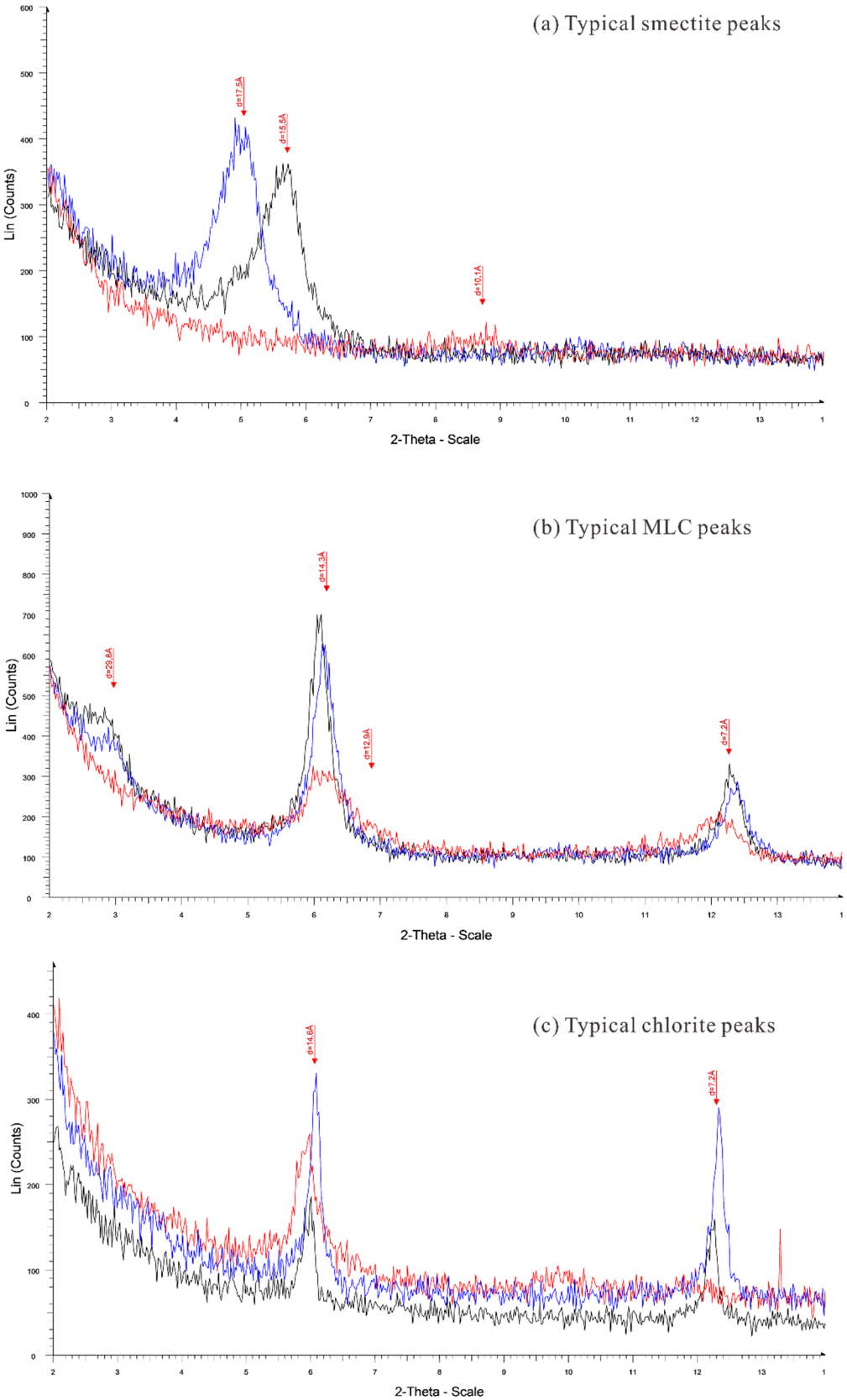

FIGURE 10: X-ray diffractometry chart showing typical behaviour of peaks for, a) Smectite zone; b) Mixed layer clay zone; and c) Chlorite zone (c) well ThG-16. The black line is produced by air drying treatment, the blue line represents glycolate treatment, and red line represents the results after heating

3.3.2 Alteration mineral sequence in well ThG-16

During the lifetime of active geothermal systems, their activity and characteristics may change. These changes can result in a shift of the activity within the region or changes in temperature, pressure, permeability, and fluid chemistry of the system. Therefore, the hydrothermal mineral assemblages that forms during different alteration events may or may not be the same. The study of hydrothermal alteration mineral sequences can be used to reconstruct the history of the system, especially space fill deposition sequences (Utami, 2011).

Mineral sequences from each thin section are observed under both a binocular and polarization microscope. Mineral sequence samples preserve more than one type of minerals filling the space in the rock. The succession of the minerals identified in well ThG-16 is mostly composed of 2 to 3 types of different minerals which are filling the veins. Single minerals were not registered as a mineral sequence but are described as a secondary mineral in the previous chapter (see Section 3.3.1). Mineral sequences from well ThG-16 generally suggest increasing formation temperature. This is explained in Figure 11 below.

Depth (md)	Rock Type	Mineral Sequence
58	mix fresh basalt, basalt olivine, tuff, pumice.	clay – chal.
100	basalt	zeo - cal
200	tuff	zeo – cal – qz.
		qz – wai.
294	Dolerite intrusion	qz - cal
480	tuff	zeo – cal.
		cal – wai.
620	basalt	qz – cal.
		chlo – ep – cal.
700	basalt	cal – qz – ep.
804	tuff	io – qz.
		ep - chlo
900	Dolerite intrusion	ep – qz – preh.
1066	basalt	cal – wai – chlo.
1110	hyaloclastite	chlo – cal.
		alb – cal.
1666	tuff breccia	qz – ep.
2250	tuff	qz - ep

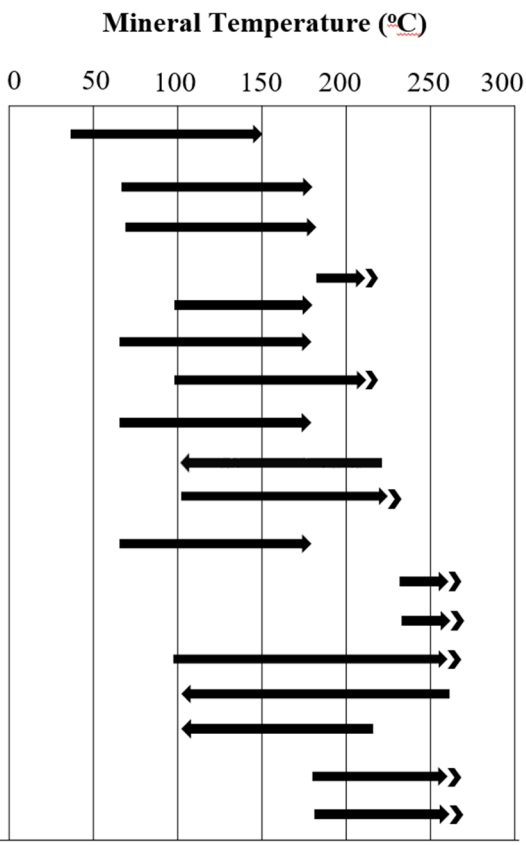

FIGURE 11: Mineral sequences encountered in space fill depositions in well ThG-16 suggest a prograde temperature trend. Mineral abbreviation refers to table 3

Figure 12 shows the photomicrograph from one of the mineral sequences encountered in well ThG-16 in the reservoir zone. This type of mineral sequence is commonly found as vein filling and vesicle precipitation product. In crossed polarized light picture (Figure 12 left), secondary quartz which is shown as grey to dark grey prismatic minerals filled the edge of a vesicle. Later, epidote with high interference colour and coarser crystal size, filled the remaining space of this vesicle. In plane polarized picture (Figure 12 right), both minerals almost have the same physical properties, especially the colour. But Epidote looks greener than secondary quartz which tends to look colourless. Moreover, Epidote has higher relief than secondary quartz in this sample picture.

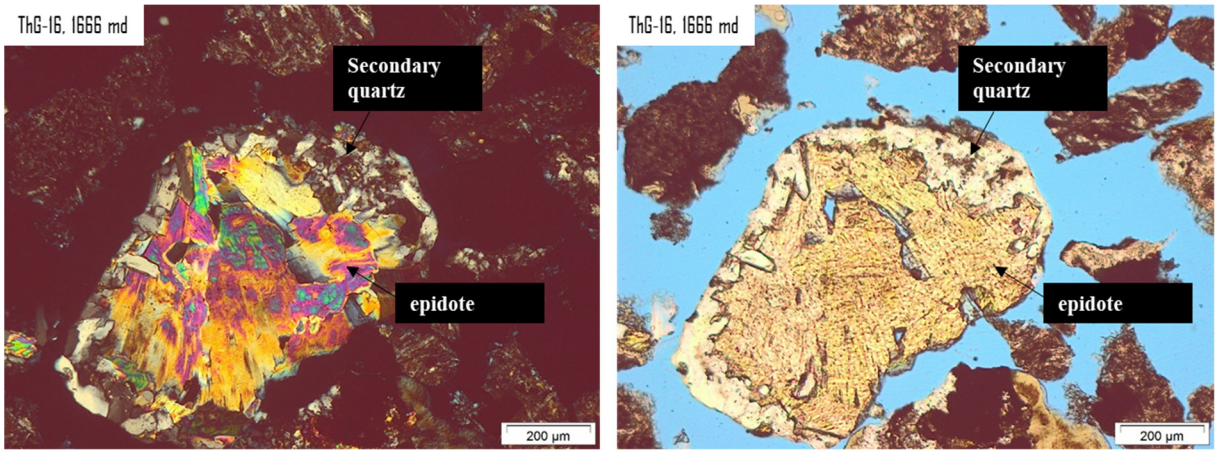

FIGURE 12: Mineral sequence of quartz to epidote from well ThG-16 indicates a prograding formation temperature at1666 m depth

Fluid inclusion analysis in well ThG-16 was conducted by Gudjónsdóttir et al. (2017b) motivated by the disappearance of epidote and the possible existence of the high-temperature zeolite laumontite at 1150 – 1160 m depth, that forms at temperatures lower than 230°C A clear mineral sample of wairakite and calcite were selected at this depth interval and 30 samples with fluid inclusions were measured.

The highest observed homogenisation temperature reaches 360°C (Figure 13). Temperature homogenisations (Th) in wairakite shows a range of 220-230°C which appeared to be associated with cracks in the crystal, and a much higher temperature which is close to the present-day temperature curve in this depth. Presumably, the lower temperature measured is younger (secondary fluid) than the higher one which is characteristic of a primary fluid (Gudjónsdóttir et al., 2017b).

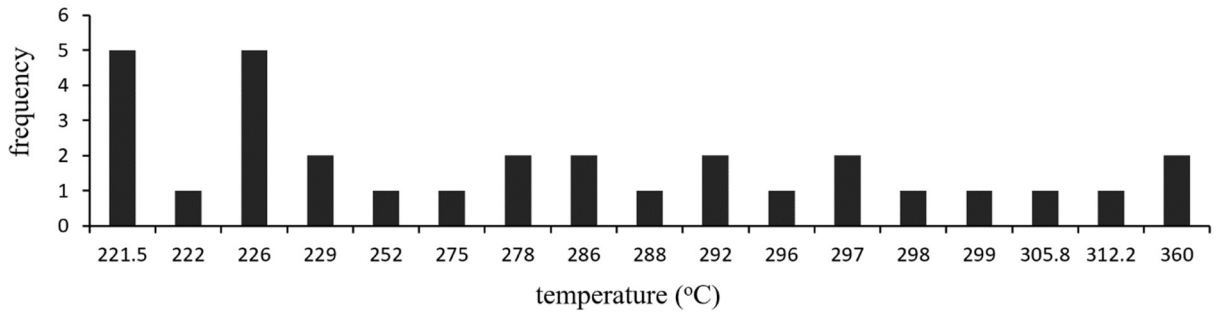

FIGURE 13: Homogenisation temperature (Th) frequency of well ThG-16 based on fluid inclusion analysis showing the most frequent Th ranging from 221 to 226°C at interval depth 1150 – 1160 m (Gudjónsdóttir et al., 2017b)

Calcite liquid generally has a higher temperature, ranging from 275 - 312°C (primary), which is just below the boiling point curve at that depth. Calcite is generally not formed at temperatures above 290°C. Measurements of fluid inclusions suggest that Th is lower than the temperature of alteration from mineral indicators at this depth (Gudjónsdóttir et al., 2017b). But at some location in the geothermal system, the temperature was in favour of the formation of epidote, prehnite, and wollastonite.

3.3.3 Alteration zone of well ThG-16

The alteration zone in well ThG-16 is divided into 5 zones based on its secondary mineral assemblages. These zonations are interpreted using mineral distributions identified by binocular, petrography, and XRD analysis. Some coarse alteration minerals could be observed under the binocular microscope but need to be confirmed with petrography analysis. The result of the petrography analysis of well ThG-16

is generally compatible with the binocular analysis. Some corrections to binocular analysis results were made when the petrography analysis suggests a different type of mineral.

Clay mineral identification confidently rely on XRD analysis. In accordance to the mineral alteration distribution in Figures 3 and 4, the binocular and petrography results agree on the clay mineral distribution. The lower temperature clay (smectite) is associated with low temperature minerals such as zeolite and chalcedony. The higher temperature clay (chlorite) appears together with high temperature mineral indicators such as epidote and actinolite. There is no ambiguity amidst each alteration zone since the distribution of mineral assemblage fits one another.

The alteration zones are displayed in Figures 3 and 4. Below a description of each zone is given:

The *fresh zone* reaches from the surface to 80 m. This zone is composed of fresh rock admix. There are no traces of hot water – rock interaction but oxidation has occurred causing the colour of the rock to appear reddish.

The *smectite zone* reaches from 80 to 170 m. This zone is characterized by low temperature clay minerals such as zeolite and smectite. Methylene blue dyed test analysis indicated high content of swelling smectite clay spiked around 42 ml/gr at 126 m and decreasing to 4.5 ml/gr at 170 m depth. This number is stable in the deeper part.

The *mixed layer clay (MLC) zone* reaches from 170 to 476 m. It is defined by the occurrence of mixed layer clay of smectite and chlorite type. The swelling smectite component is decreasing in this zone shown by the low value of MBT curve. The first occurrence of trace discontinue epidote is found in 356 - 390 m by binocular analysis.

The *epidote-chlorite zone* reaches from 476 to 1394 m. High temperature mineral assemblages such as epidote and chlorite continuously appear from 530 m onwards. These minerals are associated with albite, wollastonite, and prehnite. Low-temperature minerals such as zeolite, smectite, and chalcedony disappear in this interval.

The *epidote-chlorite actinolite zone* reaches from 1394 to 2702 m. Epidote and chlorite continuously appear from the upper part of the zone with almost the same high-temperature indicator minerals as observed in previous zones (albite, wollastonite, and prehnite) still visible from petrology analysis. This zone shows decreasing intensity of oxidation.

3.4 Televiewer and feed point analysis of ThG-16

Televiewer logging data provide fracture data in the depth interval from 850 – 2650 m. Based on Thorsteinsdóttir et al. (2018), three levels of confidence (high, medium and low) were assigned to each fracture. The method of confidence classification is described as follows:

- High confidence (score 3): Fractures which are observed >270° around the borehole, form continuous sinusoids and are picked with the least ambiguity.

- Medium confidence (score 2): Fractures which are observed 180–270° around the borehole.

- Low confidence (Score 1): Fractures that are observed only 90–180° around the borehole, very poorly resolved and difficult to select in the images. Picking of such fractures can be inaccurate, and there is a risk that these are not always real fractures.

The fracture confidence score is plotted with injectivity index, feed point size, temperature, calliper, and mineral permeability parameter in a log in Figures 14 and 15 below.

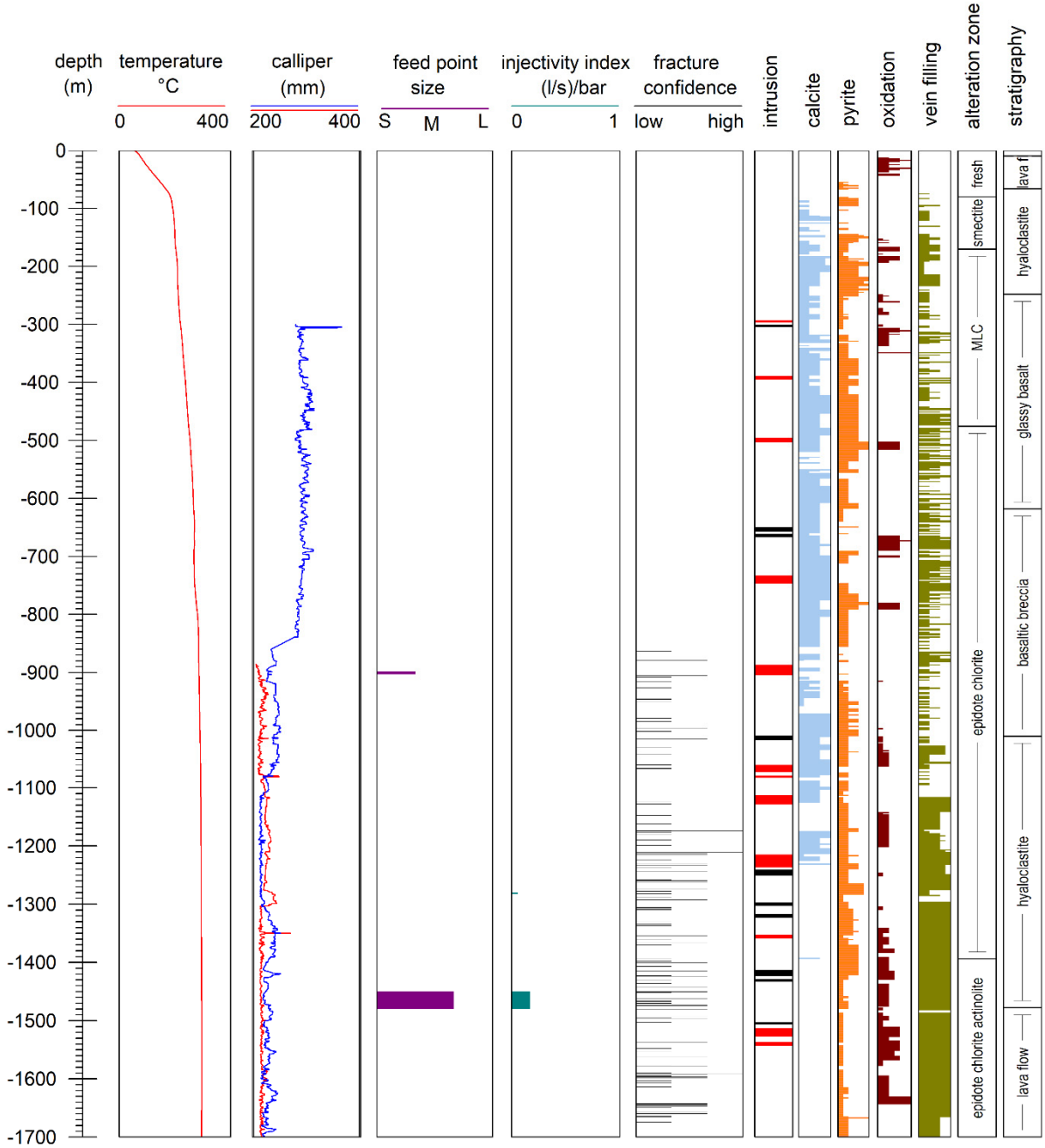

FIGURE 14: Fracture density and distribution in depth interval 0 – 1700 m

In this report, we analyse spinner analysis results from Thorsteinsdóttir et al. (2018). All the feed points found in the pressure and temperature (PT) logging are confirmed by spinner logging. At depth 1280, 1800, and 2400 m, there were no deflection in the temperature line that indicating the existence of feed point from PT chart on Figure 16. The temperature trend shows constantly linier on those depths. Nevertheless, spinner logging data strongly suggests additional feed point at 1280, 1800, and 2400 m. Spinner logging data justifies the additional feed point on Table 5. Feed point categorization classifies the rank of the feed point from PT, spinner logging, and televiewer data. The categories of feed points in well ThG-16 are summarized in Table 5.

Feed points are divided by their aperture size from small over medium to large. Fractures in ThG-16 are dominantly of small aperture size, except for depth ranges 1450 - 1480 m and 2550 - 2590 m which

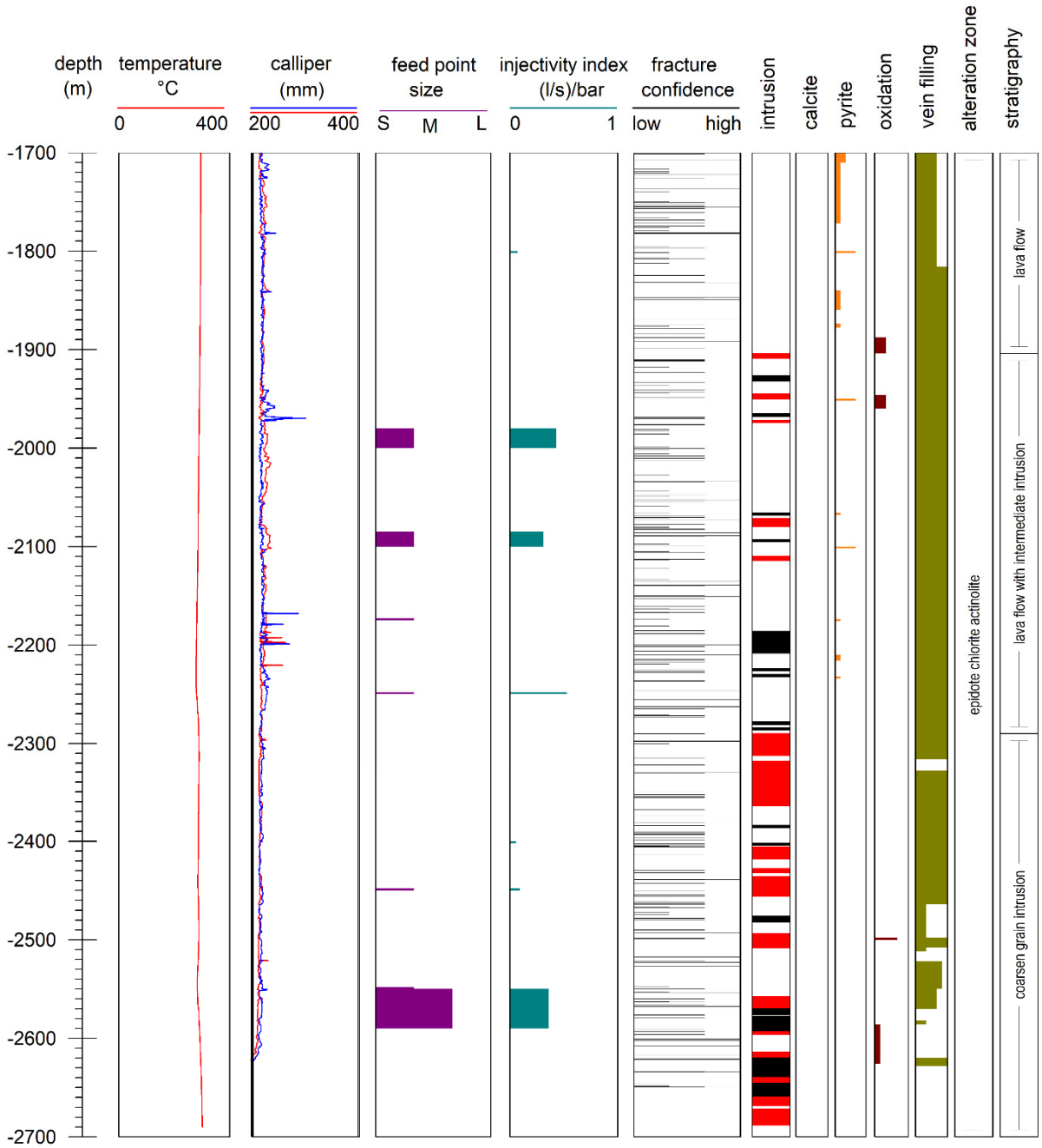

FIGURE 15: Fracture density and distribution in depth interval 1700 – 2700 m

have medium aperture size. The feed points were interpreted using televiewer image, pressure temperature logging (Figure 16), and spinner data.

Logging during injection at April the 25th (uncompleted well drilling) and May the 4th 2017 showed a temperature anomaly at around 1450 m. In shut in condition measurements, feed points were identified from recovery temperature slopes at around 2100 m, 2248 m, 2448 m, and 2550 m. Boiling conditions were obtained in the latest measurement at around 1000 m, hence the column above this depth is saturated.

The long warm up period (4 months) and its temperature trend suggests the well has low permeability. From pressure loggings, the pivot point is shown around 1300 m, indicating the best connection with the reservoir, which does not necessarily mean a feed zone.

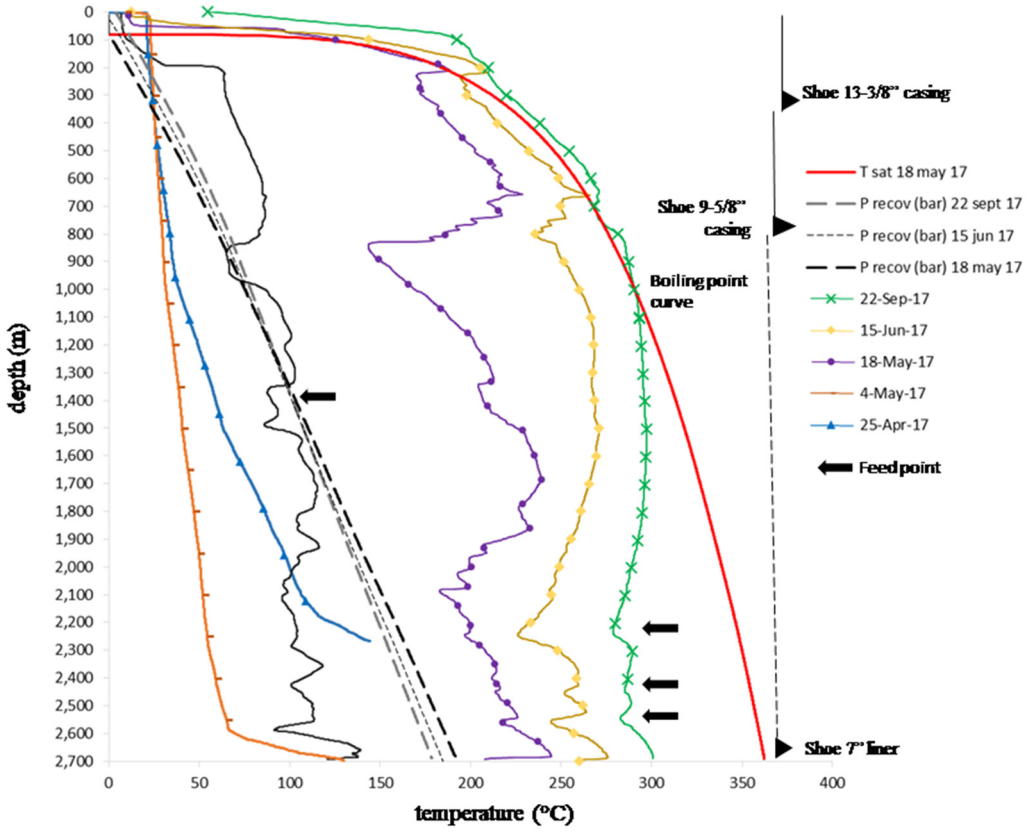

FIGURE 16: Feed point identification from pressure and temperature logging data in well ThG-16. Legend: Temperature saturation measured on 18 May 2017. Pressure recovery (bar) measured on 22 September 2017. Pressure recovery (bar) measured on 15 June 2017. Pressure recovery (bar) measured on 18 May 2017. Temperature (°C) measured on 22 September 2017. Temperature (°C) measured on 15 June 2017. Temperature (°C) measured on 18 May 2017. Temperature (°C) measured on 4 May 2017. Temperature (°C) measured on 25 April 2017

In this report, spinner analysis results from Thorsteinsdóttir et al. (2018) are analysed. All the feed points found in the pressure and temperature (PT) logging are confirmed by spinner logging. It is unseen from PT logging where the temperature trend is linear, but spinner logging suggests additional feed points at 1280, 1800, and 2400 m. Feed point categorization classifies the rank of the feed point from PT, spinner logging, and televiewer data. The categories of feed points in well ThG-16 are summarized in Table 5.

TABLE 5: Feed point category in well ThG-16 (modified from Thorsteinsdóttir, 2018). Main feed points in well ThG-16 are at 2550-2590 m, 1980-2000 m, and 1450-1480 m

Top (m)	Base (m)	Injectivity (l/s)/bar	Size category	Evidence
898	903	-	Small feed point	Temperature and Spinner logs
1280	1282	0.06	Unseen	Spinner log
1450	**1480**	**0.17**	**Medium feed point**	**Temperature and Spinner logs**
1800	1802	0.07	Unseen	Spinner log
1980	**2000**	**0.43**	**Small feed point**	**Spinner log**
2085	2100	0.31	Small feed point	Temperature and Spinner log
2173	2175	-	Small feed point	Temperature log.
2248	2250	0.53	Small feed point	Temperature and Spinner log
2400	2402	0.06	Unseen	Spinner log
2448	2450	0.09	Small feed point	Spinner log
2548	2550	-	Small feed point	Temperature and Spinner log
2550	**2590**	**0.36**	**Medium feed point**	**Temperature log**

4. DISCUSSION AND SUMMARY

Based on the analysis of this study, borehole geology of well ThG-16 is composed of lava flows and hyaloclastites from the surface down to 248 m. These layers are described as a thin fresh unaltered and a smectite zone. The highest content of swelling smectite clay appears in hyaloclastite formations. From 248 to 618 m, glassy basalt with thin layers of intrusions starts to appear. This layer is associated with a mixed layer clay zone and the first relict epidote occurs at 530 m. Alteration, pyrite abundance, and vein filling start to increase.

From 618 to 1478 m the formation is dominated by basaltic breccia and hyaloclastites. This formation indicates the top of reservoir zone where high-temperature minerals such as epidote, chlorite, albite, and prehnite become more abundant. Intrusion layers identified as crystalline basalt and dolerite are frequently found in thicker layers of up to 14 m thickness. The response of neutron, resistivity, and gamma log shows a high response conforming the intrusion.

From around 1478 to 2290 m we find lava flows with an intermediate intrusion zone below 1904 m. This zone is associated with epidote, chlorite, and actinolite. Geophysical logging (neutron, resistivity, and gamma) show increasing values due to the presence of intermediate intrusion rock together with dolerite and crystalline coarse basalt.

Below 2290 m, all the geophysical parameters show extreme high responses. This is indicating the presence of a deep-seated intermediate rock body such as an intrusion. Rock sample analysis found a dolerite and coarse grain basalt intrusion dominating this zone.

These results are in consistency with the previous analysis of well ThG-16 made by Ásgeirsdóttir, R.S et al., 2017a and 2017b and Gudjónsdóttir, S.R et al., 2017a. However, the work of this study is much more detailed, combining the different methods in order to analyse the alteration conditions in the well, as well as the lithology. With the analysis of the petrography samples (Figures 3-4) a much clearer image of the alteration mineral assembly in the well is made available. This is clearly seen with the appearance of wairakite was that was sparsely observed with binocular drill cutting analysis, but much more frequently with petrography analysis of thin sections. And for the lithological part, several dolerite intrusions were confirmed with thin section analysis of this study, that were initially mis-identified during cutting analysis during drilling of the well.

Mineral alteration in well ThG-16 shows a prograding trend in temperature with a thin layer of unaltered rocks close to the surface followed by a smectite zone. Mixed layer clay indicates a transition zone before entering the top of reservoir zone after 476 m, confirmed by epidote, wairakite, prehnite, and chlorite.

No visible high-temperature mineral was found in the depth interval from 1150 to 1160 m during drilling of ThG-16, such as epidote, prehnite, or wollastonite (Ásgeirsdóttir et al., 2017a and 2017b and Gudjónsdóttir et al., 2017a.), but in this study they are observable in the petrography analysis (sample at 1110 m) and appear together with chlorite as was identified by XRD analysis (sample at 1140 m).

The epidote chlorite actinolite zone represent a high-temperature zone below 1394 m. Despite the abundance of high-temperature indicating minerals, the results of the temperature measurement in this zone show a temperature reversal below 1600 m. This is probably the effect of cooling water inflow in the deeper part of the well. The correlation between alteration mineral geothermometers and measured recovery temperature is shown in Figure 17.

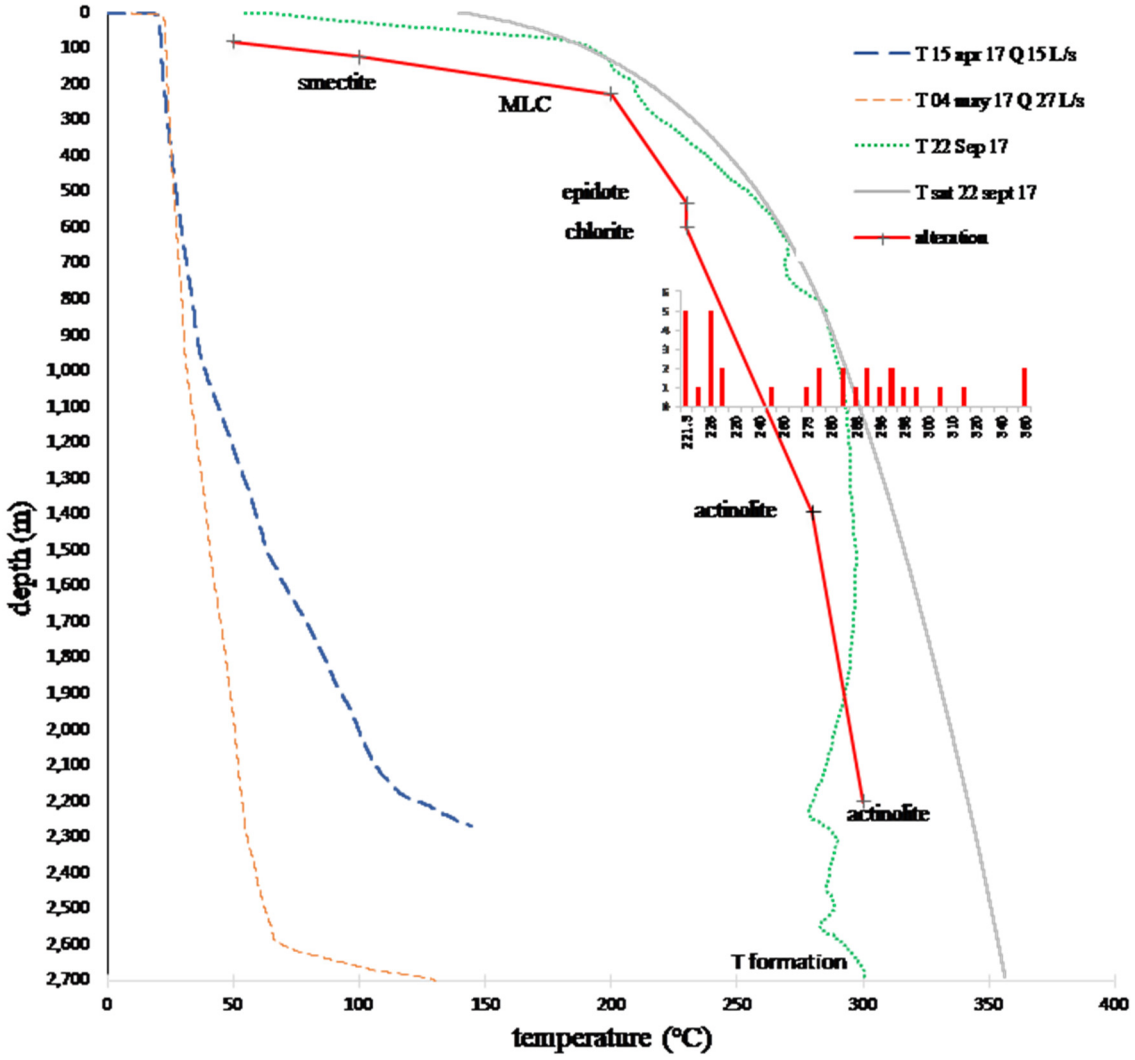

FIGURE 17: Mineral geothermometers and measured recovery temperature in well ThG-16. The profile shows the mineral association indicating high temperatures However, the reverse temperature encountered in the deeper part of the well is interpreted as a cold-water influx

5. CONCLUSIONS

The stratigraphy of well ThG-16 is composed of various volcanic rock formations from glacial and non-glacial periods, such as basaltic lava, hyaloclastite, and basaltic breccia. Between the formations, intrusion layers are commonly encountered. The intrusions consist of crystalline coarse basalt and dolerite, and in the deeper part of the well an intermediate intrusion rock body is observed.

The alteration zone is divided into five zones. From the surface to 80 m is an unaltered zone, followed by a smectite zone (80 – 170 m), a mixed layer clay zone (170 – 476 m), an epidote-chlorite zone (476 – 1394 m), and an epidote-chlorite-actinolite zone (1394 – 2700 m).

Three main feed points are observed in well ThG-16 at 2550-2590 m, 1980-2000 m, and 1450-1480 m. Well ThG-16 did not hit total loss of circulation while it was drilled which is explained by the lack of permeability. This is confirmed by the small size of fractures found in the televiewer log and the long heating up period of the well after drilling.

ACKNOWLEDGEMENTS

I would like to acknowledge Mr. Lúdvík S. Georgsson, Director, and, Mr. Ingimar G. Haraldsson, Deputy Director of the UNU-GTP, for giving me the opportunity to participating in the 6 months geothermal training program. Furthermore, thanks to Ms. Málfrídur Ómarsdóttir, Ms. Thórhildur Ísberg, Mr. Markús A.G. Wilde, and Dr. Vigdís Hardardóttir for their assistance during my study.

My sincere thanks to all my supervisors, Ms. Sylvia Rakel Gudjóndóttir, Anette K. Mortensen, Dr. Hjalti Franzson, Dr. Tobias B. Weisenberger, Mr. Sigurdur Sveinn Jónsson, and Helga Margrét Helgadóttir, for many useful discussions and advice throughout the specialisation project.

I send my gratitude to PT Pertamina Geothermal Energy (PGE) in Indonesia and my colleagues from the Exploration and Exploitation division for all the support that they have given me. To all my wonderful fellows of the UNU-GTP class of 2019, we will not stop here, see you in the future.

Special thanks go to my beloved family and friends for their encouragement and prayers during my stay in Iceland.

REFERENCES

Ásgeirsdóttir, R.S., Sigurgeirsson, M.A., Stefánsson, H.O., Ingólfsson, H., and Haraldsdóttir, S.H., 2017a: *Theistareykir – Well ThG-16. Phases 0 and 1: Drilling for surface casing down to 120 m and anchor casing down to 306 m*. ÍSOR - Iceland GeoSurvey, Reykjavík, report ÍSOR-2017/25, LV-2017-039, 89 pp.

Ásgeirsdóttir, R.S., Tryggvason, H.H., Sigurgeirsson, M.A., Pétursson, F., Vilhjálmsson, S., Gudjónsdóttir, S.R., Egilson, Th., Sveinbjörnsson, B.M., 2017b: *Theistareykir - well ThG-16. Phase 2: Drilling for production casing down to 855 m*. ÍSOR - Iceland GeoSurvey, Reykjavík, report ÍSOR-2017/38, LV-2017-050, 95 pp.

Browne, P.R.L., 1978: Hydrothermal alteration in active geothermal fields. *Annual Reviews of Earth and Planetary Science, 6,* 229-250.

Chen, P.Y., 1977: *Table of key lines on x-ray powder diffraction patterns of minerals in clays and associated rocks.* Bloomington, IN, 67 pp.

Gautason, B., Gudmundsson, Á., Hjartarson, H., Blischke, A., Mortensen, A.K., Ingimarsdóttir, A., Gunnarsson, H.S., Sigurgeirsson, M.Á., Árnadóttir, S., and Egilson, Th., 2010: Exploration drilling in the Theistareykir high-temperature field, NE-Iceland: Stratigraphy, alteration and its relationship to temperature structure. *Proceedings of the World Geothermal Congress 2010, Bali, Indonesia*, 5 pp.

Gudjónsdóttir, S.R., Sigurgeirsson, M.Á., Ásgeirsdóttir, R.S., Gudmundsdóttir, V., Tryggvason, H.H., Egilson, Th., Pétursson, F., Gunnarsson, B.S., Ingólfsson, H., Vilhjálmsson, S., and Sveinbjörnsson, B.M., 2017a: *Theistareykir - well ThG-16. Phase 3: drilling for a 7" perforated liner down to 2702 m*. ÍSOR - Iceland GeoSurvey, Reykjavík, report ÍSOR-2017/46, LV-2017-066, 213 pp.

Gudjónsdóttir, S.R., Ásgeirsdóttir, R.S., Franzson H., 2017b: *Theistareykir, well ThG-16*. ÍSOR – Iceland GeoSurvey, Reykjavík, memo 23.4.2017/SRG-RÁ-HF (brief in Icelandic), 2 pp.

Hardarson, B.S., Fitton, J.G., Ellam, R.M., and Pringle, M.S, 1997: Rift relocation - a geochemical and geochronological investigation of a paleo-rift in northwest Iceland. *Earth Planet. Sci. Lett., 153,* 181-196.

Helgadóttir, H.M., Snaebjörnsdóttir, S.Ó., Níelsson, S., Gunnarsdóttir, S.H., Matthíasdóttir, T., Hardarson, B.S., Einarsson, G.M., and Franzson, H., 2010: Geology and hydrothermal alteration in the reservoir of the Hellisheidi high temperature system, SW-Iceland. *Proceedings of the World Geothermal Congress 2010, Bali, Indonesia,* 10 pp.

Kristmannsdóttir, H., 1977: Types of clay minerals in altered basaltic rocks, Reykjanes, Iceland. *Jökull, 26* (in Icelandic with English summary), 3-39 pp.

Kristmannsdóttir, H., 1979: Alteration of basaltic rocks by hydrothermal activity at 100-300°C. In: Mortland, M.M., and Farmer, V.C. (editors), *International Clay Conference 1978*. Elsevier Scientific Publishing Co., Amsterdam, 359-367 pp.

MacKenzie, W.S., Donaldson, C.H., and Guildford C., 1982: *Atlas of igneous rocks and their textures.* Longman Group Ltd., Essex, 148 pp.

Nehler, M., Mielke, P., Bignall G., and Sass, I., 2014: New methods of determining rock properties for geothermal reservoir characterization. *Proceedings of the 19th Engineering Geology Conference with Forum for Young Engineering Geologists, Munich*, 459-466.

Reyes, A.G., 2000: *Petrology and mineral alteration in hydrothermal systems: from diagenesis to volcanic catastrophes*. UNU-GTP, Iceland, report 18-1998, 77 pp.

Saemundsson, K., 1974: Evolution of the axial rifting zone in Northern Iceland and the Tjörnes fracture zone. *Geology Society of America, Bulletin, 85-4,* 495–504.

Saemundsson, K., 1979: Outline of the geology of Iceland. *Jökull, 29,* 7-28 pp.

Saemundsson K., 2007: *Geology of the Theistareykir area*. ÍSOR – Iceland GeoSurvey, Reykjavík, report ÍSOR-07270 (in Icelandic), 23 pp.

Thompson A.J.B., and Thompson J.F.H., 1996: *Atlas of alteration; a field and petrographic guide to hydrothermal alteration minerals.* Geological Association of Canada, Canada, 119 pp.

Thorsteinsdóttir, U., Árnadóttir, S., Gautason, B., Gunnarsson, B.S., Pétursson, F., Ingimarsson, H., and Egilson., Th., 2018: *Well ThG-16. Results of televiewer imaging at the Theistareykir geothermal field, NE-Iceland*. ÍSOR - Iceland GeoSurvey, Reykjavík, report ÍSOR-2018/76, LV-2018-101, 137 pp.

Utami, P., 2011: *Hydrothermal alteration and the evolution of the Lahendong geothermal system, North Sulawesi, Indonesia*. The University of Auckland, Ph.D. thesis, 449 pp.